

Constraints on Ξ^- nuclear interactions from capture events in emulsion

E. Friedman¹ and A. Gal*¹

¹*Racah Institute of Physics, The Hebrew University, Jerusalem 91904, Israel*

(Dated: February 28, 2022)

Five $\Xi^-p \rightarrow \Lambda\Lambda$ two-body capture events in ^{12}C and ^{14}N emulsion nuclei, in which a pair of single- Λ hypernuclei is formed and identified by their weak decay, have been observed in (K^-, K^+) emulsion exposures at KEK and J-PARC. Using a $t\rho$ optical potential, we consider the combined Ξ^- atomic and nuclear cascade process, confirming that these capture events occur from Coulomb assisted $1p_{\Xi^-}$ nuclear states. Long-range ΞN shell-model correlations are found essential to achieve consistency between the ^{12}C and ^{14}N events. The resulting Ξ^- -nuclear interaction is stronger than *all* model interactions suggested in the last two decades, with $1s_{\Xi^-}$ binding energies in ^{12}C and ^{14}N exceeding 10 MeV. Implications to multi-strangeness features of dense matter are outlined.

PACS numbers:

Introduction and background. Recent two-particle correlation studies of $p\Lambda$, $\Lambda\Lambda$ and Ξ^-p pairs measured by ALICE [1–4] in pp and $p\text{-Pb}$ ultra-relativistic collisions at TeV energies have triggered renewed interest in Strangeness $\mathcal{S} \neq 0$ baryon-baryon interactions and consequences thereof to strange hadronic matter. In particular, the Ξ^-p interaction was shown to be attractive [3], in good agreement with the recent HAL-QCD lattice calculations reaching $m_\pi = 146$ MeV [5]. Understanding the strength of the $\mathcal{S} = -2$ ΞN interaction, particularly when embedded in nuclear media, is vital for resolving the Hyperon Puzzle which addresses the fate of hyperons in dense neutron-star matter [6].

Little is known from experiment on the nuclear interaction of Ξ hyperons [7, 8]. A standard reaction production is the nuclear (K^-, K^+) reaction, driven by $K^-p \rightarrow K^+\Xi^-$ strangeness exchange on protons. Owing to its large momentum transfer, the produced Ξ^- hyperons populate dominantly the quasi-free continuum region, with less than 1% expected to populate Ξ^- -nuclear bound states that decay subsequently by the $\Xi^-p \rightarrow \Lambda\Lambda$ strong-interaction capture reaction. Analysis of old emulsion events attributed to the formation of Ξ hypernuclei suggested attractive Woods-Saxon Ξ nuclear potential depth $V_{\Xi} = 21\text{--}24$ MeV [9]. While this range of values is considered sufficient for Ξ hyperons to play an active role in strange hadronic matter [10] and in neutron stars [11], somewhat smaller values follow from studies of dedicated (K^-, K^+) counter experiments: $V_{\Xi} \lesssim 20$ MeV in KEK PS-E224 [12], $V_{\Xi} \sim 14$ MeV in BNL AGS-E885 [13], both on ^{12}C , and $V_{\Xi} = 17 \pm 6$ MeV on ^9Be [14] from BNL AGS-E906 [15]. New results from the J-PARC E05 (K^-, K^+) experiment on ^{12}C are forthcoming [16]. However, no Ξ^- or $\Lambda\Lambda$ hypernuclear bound states have ever been observed unambiguously in these experiments. New, more powerful experiments by the PANDA Collab-

oration at FAIR [17], using $\bar{p}p \rightarrow \Xi^-\bar{\Xi}^+$ or $\bar{p}n \rightarrow \Xi^-\bar{\Xi}^0$ production modes, and also at BESIII [18] focusing on the $J/\psi \rightarrow \Xi^-\bar{\Xi}^+$ $O(10^{-3})$ decay branch, are likely to change this situation.

The situation is different in exposures of light-emulsion CNO nuclei to the (K^-, K^+) reaction, in which a tiny fraction of the produced high-energy Ξ^- hyperons slow down in the emulsion, undergoing an Auger process to form high- n atomic levels, and cascade down radiatively. Cascade essentially terminates, when strong-interaction capture takes over, in a 3D atomic state bound by 126, 175, 231 keV in C, N, O, respectively, shifted by less than 1 keV due to the strong interaction [19]. Capture events are recorded by observing Λ hyperon or hypernuclear decay products. Interestingly, whereas the few observed double- Λ hypernucleus production events are consistent with Ξ^- capture from atomic 3D states [8], formation of pairs of single- Λ hypernuclei requires capture from a lower Ξ^- orbit. Expecting the final two Λ hyperons in $\Xi^-p \rightarrow \Lambda\Lambda$ capture to be formed in a $S = 0$, $1s_{\Lambda}^2$ configuration, the initial Ξ^- hyperon and the proton on which it is captured must satisfy $l_{\Xi^-} = l_p$ [20] which for p -shell nuclear targets favors the choice $l_{\Xi^-} = 1$. Indeed, all two-body Ξ^- capture events, $\Xi^- + {}^A Z \rightarrow {}_{\Lambda}^{A'} Z' + {}_{\Lambda}^{A''} Z''$, to twin single- Λ hypernuclei reported from KEK and J-PARC light-emulsion K^- exposures [21–23], as listed here in Table I, are consistent with Ξ^- capture from ~ 1 MeV loosely bound $1p_{\Xi^-}$ Coulomb-assisted nuclear states. Not listed in the table are multi-body capture events that require for their interpretation undetected capture products, usually neutrons, on top of a pair of single- Λ hypernuclei. Most of these new J-PARC E07 events [24] imply Ξ^- capture from its $1s_{\Xi^-}$ ground state (g.s.) with capture rates several orders of magnitude below those for capture from the $1p_{\Xi^-}$ Coulomb-assisted excited state in each of these light-emulsion nuclear cores [25].

In Table I only the first and last listed events are uniquely assigned in terms of initial emulsion nucleus ${}^A Z$ and final single- Λ hypernuclei ${}_{\Lambda}^{A'} Z' + {}_{\Lambda}^{A''} Z''$ ground states, providing thereby a unique value of B_{Ξ^-} per each

*Corresponding author: avragal@savion.huji.ac.il

TABLE I: Reported two-body Ξ^- capture events $\Xi^- + {}^A Z \rightarrow {}^A_\Lambda Z' + {}^A_\Lambda Z''$ in light-emulsion nuclei to a pair of single- Λ hypernuclei, some in ground states, some in excited states marked by * superscripts. Fitted Ξ^- binding energies B_{Ξ^-} are listed.

Experiment	Event	${}^A Z$	${}^A_\Lambda Z' + {}^A_\Lambda Z''$	B_{Ξ^-} (MeV)
KEK E176 [21]	10-09-06	${}^{12}\text{C}$	${}^4_\Lambda\text{H} + {}^9_\Lambda\text{Be}$	0.82 ± 0.17
KEK E176 [21]	13-11-14	${}^{12}\text{C}$	${}^4_\Lambda\text{H} + {}^9_\Lambda\text{Be}^*$	0.82 ± 0.14
KEK E176 [21]	14-03-35	${}^{14}\text{N}$	${}^3_\Lambda\text{H} + {}^{12}_\Lambda\text{B}$	1.18 ± 0.22
KEK E373 [22]	KISO	${}^{14}\text{N}$	${}^5_\Lambda\text{He} + {}^{10}_\Lambda\text{Be}^*$	1.03 ± 0.18
J-PARC E07 [23]	IBUKI	${}^{14}\text{N}$	${}^5_\Lambda\text{He} + {}^{10}_\Lambda\text{Be}$	1.27 ± 0.21

event. The events fitted by assuming specific excited states ${}^A_\Lambda Z''^*$ are equally well fitted each by g.s. assignments ${}^A_\Lambda Z''$, with values of B_{Ξ^-} as high as ~ 4 MeV. Finally, the middle event is equally well fitted as a capture event in ${}^{16}\text{O}$, to ${}^3_\Lambda\text{H} + {}^{14}_\Lambda\text{C}$ with $B_{\Xi^-} = 0.46 \pm 0.39$ MeV or to ${}^4_\Lambda\text{H} + {}^{13}_\Lambda\text{C}$ with $B_{\Xi^-} = 0.40 \pm 0.27$ MeV, both consistent with Ξ^- capture from an atomic 3D state. We note that the listed Ξ^- binding energy B_{Ξ^-} values are all around 1 MeV, significantly higher than the purely-Coulomb atomic 2P binding energy values which are approximately 0.3, 0.4, 0.5 MeV in C,N,O atoms, respectively. These ~ 1 MeV B_{Ξ^-} values correspond to $1p_{\Xi^-}$ nuclear states that evolve from 2P atomic states upon adding a strong-interaction Ξ nuclear potential.

In the present work we consider the Ξ^- atomic cascade process, using a spin-independent $t\rho$ optical potential, to substantiate that $\Xi^- p \rightarrow \Lambda\Lambda$ capture indeed occurs from a Coulomb-assisted nuclear $1p_{\Xi^-}$ state in light emulsion nuclei. The strength of this Ξ -nuclear potential is determined by requiring that it reproduces a $1p_{\Xi^-}$ nuclear state in ${}^{12}\text{C}(0_{\text{g.s.}}^+)$ bound by 0.82 ± 0.15 MeV from Table I. Disregarding temporarily the $s_{\Xi^-} = \frac{1}{2}$ Pauli-spin degree of freedom, we proceed to discuss the implications of identifying the value $B_{\Xi^-} \approx 1.15 \pm 0.20$ MeV for ${}^{14}\text{N}$ from Table I with the binding energy of $\mathcal{L}^\pi = (0^-, 1^-, 2^-)$ triplet of $1p_{\Xi^-}$ nuclear states built on $J^\pi({}^{14}\text{N}_{\text{g.s.}}) = 1^+$, thereby linking the capture process to properties of the Ξ -nucleus residual interaction. This provides the most comprehensive phenomenological deduction of the Ξ -nuclear interaction from analysis of the only five Ξ^- capture events in light nuclear emulsion which have been fitted unambiguously to two-body formation of specific Λ hypernuclei, as listed in Table I. The resulting Ξ -nuclear potential, with nuclear-matter depth $V_{\Xi^-} = 24.3 \pm 0.8$ MeV, implies a significantly stronger in-medium ΞN interaction than suggested by recent model evaluations (HAL-QCD [26], EFT@NLO [27, 28], RMF [29] and Nijmegen ESC16 [30]) all of which satisfy $V_{\Xi^-} \lesssim 10$ MeV. Our results support the likelihood of Ξ^- nuclear states bound all the way down to ${}^4\text{He}$, with potentially far-reaching implications for the role of Ξ hyperons in multi-strange dense matter.

Method. The starting point in optical-potential analyses of hadronic atoms [31] is the in-medium hadron self-energy $\Pi(E, \vec{p}, \rho)$ that enters the in-medium hadron (here Ξ hyperon) dispersion relation

$$E^2 - \vec{p}^2 - m_{\Xi}^2 - \Pi(E, \vec{p}, \rho) = 0, \quad (1)$$

where \vec{p} and E are the Ξ momentum and energy, respectively, in nuclear matter of density ρ . The resulting Ξ -nuclear optical potential V_{opt} , defined by $\Pi(E, \vec{p}, \rho) = 2EV_{\text{opt}}$, enters the near-threshold Ξ^- wave equation

$$[\nabla^2 - 2\mu(B + V_{\text{opt}} + V_c) + (V_c + B)^2] \psi = 0, \quad (2)$$

where $\hbar = c = 1$. Here μ is the Ξ^- -nucleus reduced mass, B is the complex binding energy, V_c is the finite-size Coulomb interaction of the Ξ^- hyperon with the nucleus, including vacuum-polarization terms, all added according to the minimal substitution principle $E \rightarrow E - V_c$. Interaction terms negligible with respect to $2\mu V_{\text{opt}}$, i.e. $2V_c V_{\text{opt}}$ and $2BV_{\text{opt}}$, are omitted. A standard $t\rho$ form

$$V_{\text{opt}}(r) = -\frac{2\pi}{\mu} \left(1 + \frac{A-1}{A} \frac{\mu}{m_N}\right) [b_0 \rho(r) + b_1 \rho_{\text{exc}}(r)] \quad (3)$$

is used, where r is the Ξ^- -nucleus distance, $\rho = \rho_n + \rho_p$ a nuclear density distribution with r.m.s. radius taken from the corresponding charge density [32] normalized to the number of nucleons A , and $\rho_{\text{exc}} = \rho_n - \rho_p$ a neutron excess density with $\rho_n = (N/Z)\rho_p$. The complex strength parameters b_0 and b_1 (in fm) are effective ΞN isoscalar and isovector scattering lengths, respectively. The use of a Klein-Gordon type of wave equation (2) for the Ξ^- fermion rather than the Dirac equation provides an excellent approximation when $Z\alpha \ll 1$ and fine-structure effects are averaged on, as for the X-ray transitions considered here. Ξ^- nuclear spin-orbit effects are briefly mentioned below.

The form of V_{opt} given by Eq. (3) corresponds to a central-field approximation of the Ξ -nuclear interaction. Spin and isospin degrees of freedom induced by the most general two-body s -wave ΞN interaction

$$V = V_0 + V_\sigma \sigma_{\Xi} \cdot \sigma_N + V_\tau \tau_{\Xi} \cdot \tau_N + V_{\sigma\tau} \sigma_{\Xi} \cdot \sigma_N \tau_{\Xi} \cdot \tau_N, \quad (4)$$

with V s functions of $r_{\Xi N}$, are suppressed in this approach. Choosing ${}^{12}\text{C}_{\text{g.s.}}$ with isospin $I = 0$ and spin-parity $J^\pi = 0^+$ for a nuclear medium offers the advantage that only $V_0(r_{\Xi N})$ is operative in leading order since the nuclear expectation value of the other three terms in Eq. (4) vanishes. In ${}^{14}\text{N}_{\text{g.s.}}$ for example, with $I(J^\pi) = 0(1^+)$, V_σ is operative as well, adding model dependence of order $\mathcal{O}(1/A)$ to Ξ^- -nuclear potential depth values derived from capture events assigned to this emulsion nucleus. For this reason we start our analysis with the two Ξ^- - ${}^{12}\text{C}$ emulsion events listed in Table I.

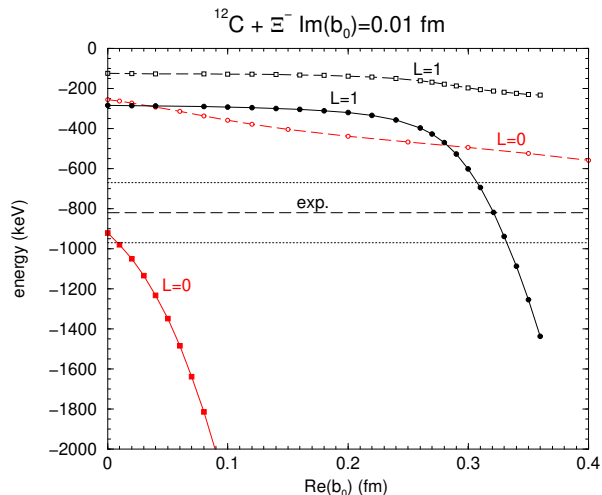


FIG. 1: Energy levels (in keV) of the lowest Ξ^- atomic states for $L=0$ (1S,2S) and $L=1$ (2P,3P) in ^{12}C as a function of the strength parameter $\text{Re } b_0$ (in fm) of the Ξ^- optical potential (3). Spin-orbit splittings of $L=1$ states are suppressed in this figure. The dashed and dotted horizontal lines mark the Ξ^- binding energy value $B_{\Xi^-} = 0.82 \pm 0.15$ MeV from Table I.

Ξ^- capture in ^{12}C . Figure 1 shows a portion of the combined atomic plus nuclear spectrum of Ξ^- in ^{12}C , $B_{\Xi^-} \leq 2$ MeV, as a function of $\text{Re } b_0$ for $\text{Im } b_0 = 0.01$ fm, corresponding to a nuclear-matter Ξ^- width $\Gamma_{\Xi^-} \approx 1.5$ MeV compatible with the weak $\Xi^- p \rightarrow \Lambda\Lambda$ transition potential from HAL QCD [5]. Plotted are the energies of the two lowest states of each orbital angular momentum $l_{\Xi^-} = 0, 1$, starting at $\text{Re } b_0 = 0$ with almost purely atomic states 1S, 2P, 2S, 3P from bottom up. Of these states the 1S state with Bohr radius about 3.8 fm is indistinguishable from a nuclear 1s state [33], and indeed it dives down in energy as soon as $\text{Re } b_0$ is made nonzero. It takes considerable strength, $\text{Re } b_0 \gtrsim 0.25$ fm, before the next atomic state, 2P with Bohr radius about 15 fm, overlaps appreciably with the $^{12}\text{C}_{\text{g.s.}}$ nuclear core, diving down in energy to become a nuclear 1p state. The higher two states that start as atomic 2S, 3P remain largely atomic as $\text{Re } b_0$ is varied in Fig. 1. Their slowly decreasing energies indicate a rearrangement of the atomic spectrum [34]: $2\text{S} \rightarrow 1\text{S}$ and $3\text{P} \rightarrow 2\text{P}$. Judging by the straight horizontal lines marking the band of values $B_{\Xi^-} = 0.82 \pm 0.15$ MeV for the two KEK E176 events listed in Table I, the figure suggests that they are compatible with a $1p_{\Xi^-}$ nuclear state corresponding to a Ξ^- -nuclear potential strength of $\text{Re } b_0 = 0.32 \pm 0.01$ fm. The sensitivity to variations of $\text{Im } b_0$ is minimal: choosing $\text{Im } b_0 = 0.04$ fm [19] instead of 0.01 fm increases $\text{Re } b_0$ by 0.01 fm to 0.33 ± 0.01 fm.

Radiative rates for E1 transitions from the Ξ^- atomic 3D state to the Ξ^- atomic 3P state, and to the $1p_{\Xi^-}$ nuclear state that started as atomic 2P state are found comparable to each other, accounting together for 7.6% of the total 3D width $\Gamma_{3\text{D}} = 3.93$ eV as obtained using

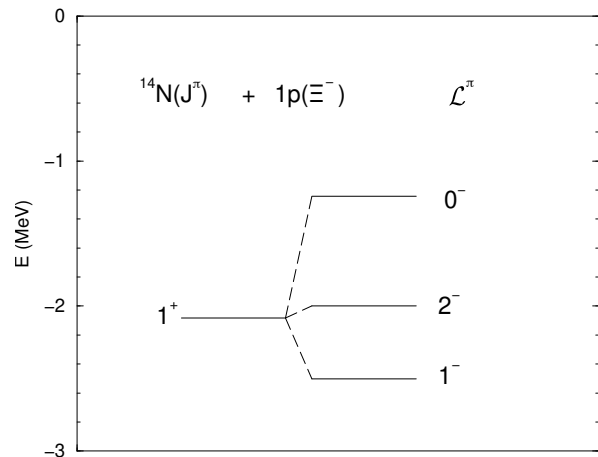


FIG. 2: Energies (in MeV) of $\mathcal{L}^\pi = (0^-, 1^-, 2^-)$ triplet of $^{14}\text{N}_{\text{g.s.}} \times 1p_{\Xi^-}$ states, split by a $Q_N \cdot Q_{\Xi}$ residual interaction (5). The $(2\mathcal{L} + 1)$ -averaged energy -2.08 ± 0.28 MeV was calculated using the same optical potential parameter b_0 that yields a $^{12}\text{C}_{\text{g.s.}} \times 1p_{\Xi^-}$ state at -0.82 ± 0.15 MeV, corresponding to the Ξ^- capture events in ^{12}C listed in Table I.

the optical potential (3). However, the subsequent $\Xi^- p \rightarrow \Lambda\Lambda$ capture will proceed preferentially from the $1p_{\Xi^-}$ nuclear state that offers good overlap between the $1p_{\Xi^-}$ and $1p_p$ valence-proton orbits. Since the final $1s_{\Lambda}^2$ configuration has $J_f = 0$, and the p -shell protons in ^{12}C are mostly in $j = \frac{3}{2}$ orbits, the requirement $J_i = J_f = 0$ imposes $j_{\Xi^-} = \frac{3}{2}$ on the spin-orbit doublet members of the $1p_{\Xi^-}$ state. The shift of this $1p_{\Xi^-}(\frac{3}{2})$ sub level from the $1p_{\Xi^-}$ $(2j + 1)$ -average is estimated, based on the 152 keV $1p_{\Lambda}$ spin-orbit splitting observed in ^{13}C [35] to be less than 100 keV upward [36] and, hence, within the 0.15 MeV listed uncertainty introduced here for the position of the $(2j + 1)$ -averaged $1p_{\Xi^-}$ state.

Spectroscopy of $^{14}\text{N}_{\text{g.s.}} \times 1p_{\Xi^-}$ states. Having derived the strength parameter $\text{Re } b_0 = 0.32 \pm 0.01$ fm of V_{opt} by fitting it to $B_{\Xi^-}^{1p}(^{12}\text{C}) = 0.82 \pm 0.15$ MeV, we apply this optical potential to ^{14}N where it yields $B_{\Xi^-}^{1p}(^{14}\text{N}) = 2.08 \pm 0.28$ MeV, considerably higher than the value $B_{\Xi^-} = 1.15 \pm 0.20$ MeV obtained from the three events assigned in Table I to Ξ^- capture in ^{14}N . However, this calculated $B_{\Xi^-}^{1p}(^{14}\text{N})$ corresponds to a $(2\mathcal{L} + 1)$ -average of binding energies for a triplet of states $\mathcal{L}^\pi = (0^-, 1^-, 2^-)$ obtained by coupling a $1p_{\Xi^-}$ state to $J^\pi(^{14}\text{N}_{\text{g.s.}}) = 1^+$, as shown in Fig. 2. The splitting of these triplet states is discussed below. Effects of Ξ^- Pauli spin, $s_{\Xi^-} = \frac{1}{2}$, are introduced at a later stage.

The construction of the $^{14}\text{N}_{\text{g.s.}} \times 1p_{\Xi^-}$ spectrum in Fig. 2 follows a similar $^{12}\text{C}(2^+; 4.44 \text{ MeV}) \times 1p_{\Lambda}$ spectrum construction in ^{13}C [37]. The energy splittings marked in the figure are obtained from a spin-independent Wigner-force residual interaction between a p -shell Ξ hyperon and p -shell nucleons, expressed in terms of a shell-model

(SM) quadrupole-quadrupole residual interaction,

$$V_{\text{res}}(\Xi N) = F_{\Xi N}^{(2)} Q_N \cdot Q_{\Xi}, \quad Q_B = \sqrt{\frac{4\pi}{5}} Y_2(\hat{r}_B), \quad (5)$$

where $F^{(2)}$ is the corresponding Slater integral [38]. A representative value of $F_{\Xi N}^{(2)} = -3$ MeV is used here, smaller than the value $F_{\Lambda N}^{(2)} = -3.7$ MeV established empirically for p -shell Λ hypernuclei [39], in accordance with a ΞN strong interaction somewhat weaker than the ΛN strong interaction (see next section). Finally, a single 3D_1 ${}^{14}\text{N}_{\text{g.s.}}$ SM component providing a good approximation to the full SM intermediate-coupling g.s. wavefunction [40] was assumed in the present evaluation.

Fig. 2 exhibits a triplet of ${}^{14}\text{N}_{\text{g.s.}} \times 1p_{\Xi^-}$ levels, spread over more than 1 MeV. The least bound triplet state, with $\mathcal{L}^\pi = 0^-$, is shifted upward by 0.84 MeV from the $(2\mathcal{L} + 1)$ -averaged position at -2.08 ± 0.28 MeV to $E(0^-) = -1.24 \pm 0.28$ MeV. This is consistent with the averaged position $\bar{E} = -1.15 \pm 0.20$ MeV of the three Ξ^- ${}^{14}\text{N}_{\text{g.s.}}$ capture events listed in Table I. We are not aware of any good reason why capture has not been seen from the other two states with $\mathcal{L}^\pi = 1^-, 2^-$. This may change when more events are collected at the next stage of the ongoing J-PARC E07 emulsion experiment.

Introducing Pauli spin, $s_{\Xi^-} = \frac{1}{2}$, the total angular momentum of the uppermost level marked 0^- in Fig. 2 becomes $J^\pi = \frac{1}{2}^-$, but its position is unaffected by spin-orbit and spin-spin interactions. Each of the other two levels in Fig. 2 splits into a doublet $J = \mathcal{L} \pm \frac{1}{2}$ whose $(2J + 1)$ -average remains in the unsplit position. These splittings are not expected to exceed about 0.5 MeV, based on estimates of $l_{\Xi^-} \cdot s_{\Xi^-}$ spin-orbit [36] and of $s_N \cdot s_{\Xi^-}$ spin-spin contributions, the latter estimated by using the HAL-QCD [5] volume integral of $V_\sigma(r_{\Xi N})$ relative to that of $V_0(r_{\Xi N})$, Eq. (4). Incorporating these spin splittings into the $\mathcal{L}^\pi = (0^-, 1^-, 2^-)$ triplet in Fig. 2 keeps the $\mathcal{L}^\pi = 0^-$ state of interest, which has become $J^\pi = \frac{1}{2}^-$, well separated by at least 0.5 MeV from the rest of the split states.

Ξ nuclear potential depth and $1s_{\Xi^-}$ states. So far we have considered $1p_{\Xi^-}$ nuclear states using a strength parameter $\text{Re } b_0 = 0.321 \pm 0.010$ fm, Eq. (3), fitted to the Ξ^- capture events in ${}^{12}\text{C}$ listed in Table I. In the limit $A \rightarrow \infty$, $\rho(r) \rightarrow \rho_0 = 0.17$ fm $^{-3}$, this implies a nuclear-matter value $V_{\Xi^-} = 24.3 \pm 0.8$ MeV for the Ξ -nuclear potential depth, in accordance with the extraction of V_{Ξ^-} from old emulsion events [9] but exceeding considerably other values reviewed in the Introduction. One expects then the Ξ^- hyperon to form bound states also in lighter core nuclei.

Ξ^- $1s$ binding energies and widths calculated solving Eq. (2) are listed in Table II for several $N = Z$ core nuclei ${}^AZ(T = 0)$ from ${}^{14}\text{N}$ down to ${}^4\text{He}$, plus ${}^{11}\text{B}(T = \frac{1}{2})$ which requires, in addition to the common isoscalar strength

TABLE II: Binding energy $B_{\Xi^-}^{1s}$ and width $\Gamma_{\Xi^-}^{1s}$ values for core nuclei ${}^AZ(J_c)$ with g.s. spin J_c , calculated by solving Eq. (2) with $b_0 = 0.321 + i0.010$ fm and (for the only $T \neq 0$ core nucleus ${}^{11}\text{B}$) $b_1 = -0.137$ fm in V_{opt} (3). A finite-size Coulomb interaction V_c was included. Spin-spin splittings $\Delta_{\Xi^-}^{1s} = E(J = J_c + \frac{1}{2}) - E(J = J_c - \frac{1}{2})$ for $J_c \neq 0$ states are listed in the last line, see text. Energies are given in MeV.

	${}^{14}\text{N}(1)$	${}^{12}\text{C}(0)$	${}^{11}\text{B}(\frac{3}{2})$	${}^{10}\text{B}(3)$	${}^6\text{Li}(1)$	${}^4\text{He}(0)$
$B_{\Xi^-}^{1s}$	12.6	10.7	9.2	8.1	1.9	2.4
$\Gamma_{\Xi^-}^{1s}$	1.07	0.98	0.95	0.81	0.25	0.53
$\Delta_{\Xi^-}^{1s}$	0.30	-	-0.21	-0.41	-0.58	-

parameter $b_0 = 0.321 + i0.010$ fm in V_{opt} , Eq. (3), also a nonzero value of the isovector strength parameter b_1 . We used the HAL-QCD [5] volume integral of $V_\tau(r_{\Xi N})$ relative to that of $V_0(r_{\Xi N})$, Eq. (4), to estimate b_1 relative to b_0 , thereby deriving a value $b_1 = -0.137$ fm. The resulting value $B_{\Xi^-}^{1s}$ (${}^{11}\text{B}$) listed in the table is lower by almost 600 keV than the value obtained upon disregarding b_1 .

The table demonstrates a steady decrease of $B_{\Xi^-}^{1s}$ and $\Gamma_{\Xi^-}^{1s}$ down to ${}^6\text{Li}$. Interestingly, the ${}^4\text{He}$ corresponding values are larger than those for ${}^6\text{Li}$, reflecting a denser ${}^4\text{He}$ core nucleus. All listed $1s_{\Xi^-}$ g.s. levels remain bound also when the finite-size Coulomb interaction V_c is removed, with $B_{\Xi^-}^{1s}$ (${}^4\text{He}$) less by 1.25 MeV and $B_{\Xi^-}^{1s}$ (${}^{14}\text{N}$) by 4.02 MeV than the listed corresponding values that include V_c . In addition to binding energies and widths, Ξ^- spin splittings are listed in the last line of the table for $J_c \neq 0$ core nuclei, making the same sort of estimate made for spin-spin splittings in Ξ^- - ${}^{12}\text{C}$. The spectroscopic part of this calculation is identical with that reviewed in Ref. [40] to calculate Λ hypernuclear spin splittings. Other potential sources of Ξ^- spin splittings that are relevant in Λ hypernuclei, such as tensor or induced spin-orbit forces, are likely to be considerably weaker than evaluated in Ref. [41] for Λ hypernuclei and are suppressed here. The Ξ^- spin splittings listed in Table II are all well below the 1 MeV scale which roughly corresponds to the increment of $B_{\Xi^-}^{1s}$ per unit A .

Finally, we note that according to Table II the $(2J + 1)$ -averaged $1s_{\Xi^-}$ g.s. is bound in ${}^{11}\text{B}$ by over 9 MeV. This strongly contrasts with statements in the literature, e.g. [8], that a $1s_{\Xi^-}$ state bound by about 5 MeV is implied by the BNL AGS-885 (K^-, K^+) experiment on ${}^{12}\text{C}$ [13]. In fact, its poor resolution prevents making any such conclusive statement.

Summary. In conclusion we have shown that all five light nuclear emulsion events identified in KEK and J-PARC K^- exposure experiments as two-body Ξ^- capture in ${}^{12}\text{C}$ and ${}^{14}\text{N}$ into two single- Λ hypernuclei correspond to capture from $1p_{\Xi^-}$ Coulomb-assisted bound states calculated using a *common* strength parameter $t\rho$ optical potential. Long-range ΞN shell-model

correlations were essential in making the ^{14}N events consistent with the ^{12}C events. Earlier attempts to explain these data missed this point, reaching thereby somewhat different conclusions [42–45]. Predicted then are $1s_{\Xi^-}$ states bound by over 10 MeV in ^{12}C and ^{14}N , substantially deeper than the $1s_{\Xi^-}$ states claimed by the very recent J-PARC E07 report of multi-body capture events [24]. The Ξ nuclear-matter potential depth derived here, $V_{\Xi} \approx 24$ MeV, is considerably larger than values well below 10 MeV derived from recent LQCD and EFT ΞN potentials [26, 28]. While this apparent disagreement deserves a more detailed discussion, it does not necessarily mean that the underlying two-body ΞN interaction models in Refs. [5, 27] are at fault.

A strong Ξ -nuclear interaction, such as derived here, may also have far-reaching implications to strange hadronic matter [10] and particularly to dense neutron star matter [11]. In the latter case a strong Ξ -nuclear interaction might cause a faster depletion of Λ hyperons by $\Lambda\Lambda \rightarrow \Xi^-p$, a process inverse to the Ξ^- capture reaction considered in the present work. More work is necessary in this direction.

The work of EF and AG is part of a project funded by the European Union’s Horizon 2020 research & innovation programme, grant agreement 824093.

-
- [1] S. Acharya *et al.* (ALICE Collaboration), Phys. Rev. C **99**, 024001 (2019).
- [2] S. Acharya *et al.* (ALICE Collaboration), Phys. Lett. B **797**, 134822 (2019).
- [3] S. Acharya *et al.* (ALICE Collaboration), Phys. Rev. Lett. **123**, 112002 (2019).
- [4] S. Acharya *et al.* (ALICE Collaboration), Nature **588**, 232 (2020).
- [5] K. Sasaki *et al.* (HAL QCD Collaboration), Nucl. Phys. A **998**, 121737 (2020).
- [6] L. Tolos, and L. Fabbietti, Prog. Part. Nucl. Phys. **112**, 103770 (2020).
- [7] A. Gal, E.V. Hungerford, and D.J. Millener, Rev. Mod. Phys. **88**, 035004 (2016).
- [8] E. Hiyama, and K. Nakazawa, Annu. Rev. Nucl. Part. Sci. **68**, 131 (2018).
- [9] C.B. Dover, and A. Gal, Ann. Phys. **146**, 309 (1983).
- [10] J. Schaffner-Bielich, and A. Gal, Phys. Rev. C **62**, 034311 (2000), and references cited therein to earlier work by J. Schaffner *et al.*
- [11] S. Weissenhorn, D. Chatterjee, and J. Schaffner-Bielich, Nucl. Phys. A **881**, 62 (2012).
- [12] T. Fukuda *et al.* (KEK PS-E224), Phys. Rev. C **58**, 1306 (1998).
- [13] P. Khaustov *et al.* (BNL AGS-E885), Phys. Rev. C **61**, 054603 (2000).
- [14] T. Harada, and Y. Hirabayashi, Phys. Rev. C **103**, 024605 (2021).
- [15] J.K. Ahn *et al.* (BNL AGS-E906), Phys. Rev. Lett. **87**, 132504 (2001).
- [16] T. Nagae *et al.* (J-PARC E05), AIP Conf. Proc. **2130**, 020015 (2019). A considerably improved resolution is planned for the E70 version of this experiment.
- [17] J. Pochodzalla *et al.* (for the PANDA Collaboration), JPS Conf. Proc. **17**, 091002 (2017).
- [18] C.Z. Yuan, and M. Karliner, arXiv:2103.06658 [hep-ex].
- [19] C.J. Batty, E. Friedman, and A. Gal, Phys. Rev. C **59**, 295 (1999).
- [20] D. Zhu, C.B. Dover, A. Gal, and M. May, Phys. Rev. Lett. **67**, 2268 (1991).
- [21] S. Aoki *et al.* (KEK PS-E176), Nucl. Phys. A **828**, 191 (2009), and earlier E176 reports cited therein.
- [22] H. Nakazawa *et al.* (KEK PS-E373), Prog. Theor. Exp. Phys. **2015**, 033D02 (2015).
- [23] S.H. Hayakawa *et al.* (J-PARC E07), Phys. Rev. Lett. **126**, 062501 (2021).
- [24] M. Yoshimoto *et al.* (J-PARC E07), arXiv:2103.08793 [nucl-ex].
- [25] T. Yamada, and K. Ikeda, Phys. Rev. C **56**, 3216 (1997).
- [26] T. Inoue (for the HAL QCD Collaboration), AIP Conf. Proc. **2130**, 020002 (2019).
- [27] J. Haidenbauer, and U.-G. Meißner, Eur. Phys. J. A **55**, 23 (2019).
- [28] M. Kohno, Phys. Rev. C **100**, 024313 (2019).
- [29] T. Gaitanos, and A. Choroizidou, Nucl. Phys. A **1008**, 122153 (2021).
- [30] M.M. Nagels, Th.A. Rijken, and Y. Yamamoto, Phys. Rev. C **102**, 054003 (2020).
- [31] E. Friedman, and A. Gal, Phys. Rep. **452**, 89 (2007).
- [32] I. Angeli, and K.P. Marinova, At. Data Nucl. Data Tables **99**, 69 (2013).
- [33] Nuclear single-particle (s.p.) states are denoted by lower-case letters: $1s, 1p, 1d, \dots$ for the lowest l values, in distinction from capital letters for atomic s.p. states: $1S, 2P, 3D, \dots$ for the lowest L values.
- [34] A. Gal, E. Friedman, and C.J. Batty, Nucl. Phys. A **606**, 283 (1996).
- [35] S. Ajimura *et al.* (BNL AGS-E929), Phys. Rev. Lett. **86**, 4255 (2001).
- [36] J. Mareš, and B.K. Jennings, Phys. Rev. C **49**, 2472 (1994).
- [37] E.H. Auerbach, A.J. Baltz, C.B. Dover, A. Gal, S.H. Kahana, L. Ludeking, and D.J. Millener, Phys. Rev. Lett. **47**, 1110 (1981); Ann. Phys. **148**, 381 (1983), where values of $-F_{\Lambda N}^{(2)} = 3.0 - 3.4$ MeV were proposed.
- [38] A. de-Shalit, I. Talmi, *Nuclear Shell Theory* (AP, New York, 1963).
- [39] R.H. Dalitz, and A. Gal, Ann. Phys. **131**, 314 (1981).
- [40] D.J. Millener, in *Topics in Strangeness Nuclear Physics*, Edited by P. Bydžovský, A. Gal, and J. Mareš, Lecture Notes in Physics **724**, 31-79 (Springer, Heidelberg, 2007).
- [41] D.J. Millener, Nucl. Phys. A **881**, 298 (2012). Note that in $^{11}\text{B}(T \neq 0)$ the $V_{\sigma\tau}$ term, Eq. (4), induces further spin splitting that keeps in line with the estimate made here. Details are given elsewhere.
- [42] M. Yamaguchi, K. Tominaga, Y. Yamamoto, and T. Ueda, Prog. Theor. Phys. **105**, 627 (2001).
- [43] E. Hiyama, Y. Yamamoto, and H. Sagawa, Phys. Scr. **91**, 093001 (2016).
- [44] T.T. Sun, E. Hiyama, H. Sagawa, H.-J. Schulze, and J. Meng, Phys. Rev. C **94**, 064319 (2016).
- [45] Y. Jin, X.-R. Zhou, Y.-Y. Cheng, and H.-J. Schulze, Eur. Phys. J. A **56**, 135 (2020).